The 2009 IEEE/RSJ International Conference on
Intelligent Robots and Systems
October 11-15, 2009 St. Louis, USA

Development of a Miniature Self-stabilization Jumping Robot

Jianguo Zhao, Ruiguo Yang, Ning Xi, Bingtuan Gao, Xinggang Fan, Matt W. Mutka, and Li Xiao

***Abstract*— We present the design and implementation of a new jumping robot for mobile sensor network. Unlike other jumping robots, the robot is based on a simple two-mass-spring model. After we throw it on ground, it can stabilize itself and then jump once. The detailed mechanism design including the load holding and self-stabilization are presented. Jumping heights and distances with different robot weights are measured and compared with calculated values from the two-mass-spring model.**

I. INTRODUCTION

Mobile sensor network with self-deployment and self-repair abilities has attracted much research attention compared with its static counterpart in recent years. It consists of nodes with capabilities of communication, sensing, computation, and locomotion. In fact, these nodes can be considered as robots with sensors. While the robots provide the locomotion capability, the sensors perform the other functions. The robots for this application are always assumed as wheeled robots such as in [1]. If, however, the environment is rugged terrain with obstacles that wheeled robots cannot overcome, jumping robots are preferred. Furthermore, jumping robots are more economical than wheeled ones due to their compact size [2]. The disadvantage is the less movement accuracy because of its discrete jumping nature [3]. Nevertheless, since position accuracy is not critical in typical sensor network applications such as area coverage, this disadvantage can be ignored.

In this paper, we aim to present the development of a jumping robot for this application. The ultimate goal is to build a robot that can repeatedly perform the following motion sequences: first of all, the robot orients its body into the desired jumping direction, then the robot jumps with a certain takeoff angle, and finally, after landing on the ground, it can self-stabilize for the next jump. As our first prototype, we just want to achieve part of the goal: randomly throw the robot on the ground, the robot can stabilize itself and jump once after receiving a signal. Based on this goal and the application, the design specifications can be determined as follows: the robot's weight should be less than $50g$, jump height should be greater than $15cm$, and jump distance should be greater than $10cm$. Under these specifications, we have built the prototype as shown in Fig. 1(a) and the jumping state is shown in Fig. 1(b), where three of four robots, labeled by circles, are in the air.

Many jumping robots have been designed these years. In most of the prototypes, spring is used to store energy and then the energy is released to make the robot thrust. The examples include the Minimalist hopper [2], 7g [4], Grillo [5], Jollbot [6], Mini-Whegs [7], and Scout [8]. Although there exist other energy storage methods such as compression air [9] and combustion [10], the spring based approach is suitable for our application because of the size and weight limits.

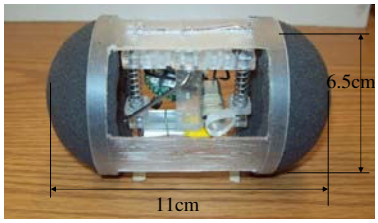

(a) Jumping robot prototype

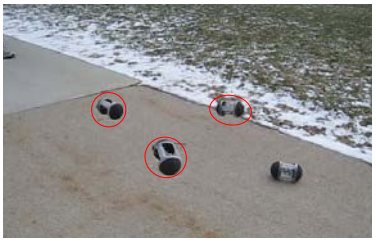

(b) Jumping state

Fig. 1. The first prototype of jumping robot

The rest of paper is organized as follows. In section II, mathematical model of the jumping robot is established, serving as guidance for our design. Then the detailed design is explained in section III. The experimental results are given and compared with the theoretical calculations in section IV. Finally, we conclude the paper and outline future works.

II. MATHEMATICAL MODELS

For most of the spring based jumping robots, the leg is a four bar mechanism such as the 7g [4], Mini-Wheg [7], and Grillo [5]. Nevertheless, a simpler method using the compression spring can be adopted. In this case, the leg and body of the robot are simply connected by a compression spring. In this section, we model this method by a two-mass-spring system, a lower mass and an upper mass connected by a spring, to analyze the jumping process.

This research is supported in part by NSF grant CNS-0721441.

Jianguo Zhao, Ruiguo Yang, Ning Xi, and Bingtuan Gao are with Department of Electrical and Computer Engineering, Michigan State University, MI, USA. zhaojia1@msu.edu, yangruig@msu.edu, xin@egr.msu.edu, carlgao@msu.edu

Xinggang Fan is with College of Information Engineering, Zhejiang University of Technology, Zhejiang, P. R. China. fanxghangzhou@hotmail.com

Matt W. Mutka and Li Xiao are with the Department of Computer Science and Engineering, Michigan State University, East Lansing, MI 48824, USA. {mutka, lxiao}@cse.msu.edu

For spring based jumping, it is expected that the energy stored in the spring should be converted to the kinetic energy of the jumping robot as much as possible. This can be evaluated by conversion efficiency η as defined in [2]:

$$\eta = \frac{\text{kinetic energy at takeoff}}{\text{energy stored in compressed medium}}$$

In this section, the conversion efficiency will also be analyzed based on proposed model.

A. Vertical Model

Suppose two masses m_1 and m_2 are connected by a spring with a constant K as shown in Fig. 2. In the initial state, the system is subjected to an external force F. After the force is removed, the system will begin to jump. Although the system will typically jump up and down for several times, only the first cycle is important since the largest height occurs in this cycle. The process of the first cycle can be divided into four steps listed as follows and shown in Fig. 2.

1 The upper mass moves upward with an increasing velocity, while the lower mass stays still. Meanwhile, the upward spring force f will decrease. This step ends until $f = m_2 g$.

2 The upper mass moves upward with a decreasing velocity, while the lower mass still stays on the ground. Spring force will first decrease to zero, reverse its direction, and then increase. This step ends when $f = m_1 g$.

3 The lower mass begins to move upward. The two masses will perform a harmonic motion. This step lasts until the system reaches the largest height.

4 The system begins to fall down, and the step ends until the lower mass reaches the ground.

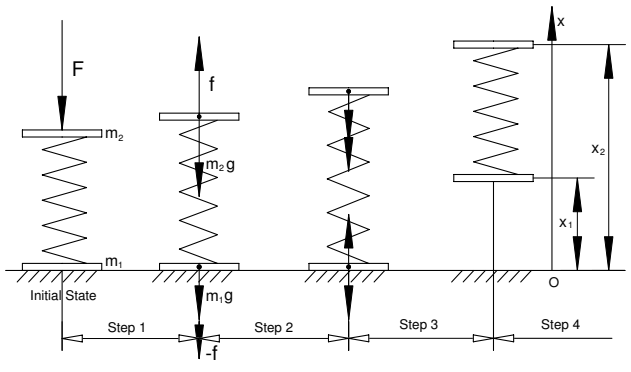

Fig. 2. Four steps for vertical two-mass-spring system

Suppose the length of the spring at rest is l. Establish the coordinate frame as shown in Fig. 2. Assume the heights of two masses are both zero, then the compression (positive) or extension (negative) length is $\Delta x = l - (x_2 - x_1)$. Neglect the air resistance and suppose the spring can both compress and extend with the same constant, we have:

$$m_1 \ddot{x}_1 = -m_1 g - K\Delta x \tag{1}$$

$$m_2 \ddot{x}_2 = -m_2 g + K\Delta x \tag{2}$$

Plug Δx into above equation, we have:

$$\ddot{x}_1 = -\frac{K}{m_1}x_1 + \frac{K}{m_1}x_2 - g - \frac{Kl}{m_1} \tag{3}$$

$$\ddot{x}_2 = \frac{K}{m_2}x_1 - \frac{K}{m_2}x_2 - g + \frac{Kl}{m_2} \tag{4}$$

These two equations can be converted to four first order inhomogeneous differential equations with initial values corresponding to the position and velocity of two masses at the initial state of step 3. The position and velocity for m_1 are both zero, while for m_2 they can be obtained by energy conservation. The solution to above equations is the governing equation of motion during the first cycle. At the end of step 3 (the peak height), the velocity of the upper mass should be zero. Using this condition, we can obtain the jumping height from the governing equations. The equations, however, are quite complicated, and a simplified model is needed to derive the jumping height.

Intuitively, if we want the robot to jump as high as possible, we should make the robot as light as possible and use a spring with a large constant which can store more energy for a given compression length. For example, let jumping height be $h = 15cm$, the weight of the robot be $m = 50g$, and the compression length of the spring be $\Delta x = 10mm$ (limited by the robot size), then we have:

$$\frac{1}{2}K\Delta x^2 > mgh$$

From this inequality, we get $K > 1470N/m$. If all the weight of $50g$ are applied to the spring, it will only have a $0.34mm$ compression length. Based on this observation, the four steps in Fig. 2 can be reduced to three steps: first, the upper mass moves upward until the spring extends to original length because the weight of the upper mass is negligible with respect to the spring; second, both masses move upward together with a same speed because the spring can be considered as rigid compared with the two masses; third, the system falls down.

Therefore, at the end of new step 1, we have:

$$F = K\Delta x \tag{5}$$

$$\frac{1}{2}K\Delta x^2 = \frac{1}{2}m_2 v_2^2 \tag{6}$$

where v_2 is the speed of upper mass. Hence

$$v_2 = \frac{F}{\sqrt{Km_2}} = \sqrt{\frac{K}{m_2}}\Delta x$$

At the start of new step 2, by conservation of momentum, we have:

$$m_2 v_2 = (m_1 + m_2)v$$

where v is the same takeoff speed for both masses, and

$$v = \frac{\sqrt{m_2 K}}{m_1 + m_2}\Delta x \tag{7}$$

Then the two masses will move upward with this same speed v. Thus, the kinetic energy at takeoff is:

$$E = \frac{m_2 K\Delta x^2}{2(m_1 + m_2)} = \frac{1}{r+1}E_0$$

where $r = m_1/m_2$ is the mass ratio of the two masses and $E_0 = K\Delta x^2/2$ is the energy stored in the spring in the initial state. Thus we have the conversion efficiency as:

$$\eta = \frac{1}{r+1} \tag{8}$$

From (8), if $r = 0$, then all the spring energy will be converted to the potential energy, while if $r \neq 0$, some spring energy will be lost. Therefore, we should make the mass ratio as small as possible. The above takeoff energy will be converted to the potential energy if no air resistance is considered, and we can get the jumping height by conservation of energy:

$$h = \frac{\eta E_0}{(m_1+m_2)g} \tag{9}$$

In order to achieve a jumping height as large as possible, from (8) and (9), we can formulate three design guidances as follows:

1) Maximize the stored energy E_0;
2) Minimize the total weight of the two masses m_1+m_2;
3) Minimize the mass ratio r.

B. Tilted Model

Aside from jumping height, jumping distance is also a critical index to evaluate the robot's performance. To analyze the jumping distance, the tilted model for the two-mass-spring system is developed as shown in Fig. 3. In this case, we also use the simplified three steps in the vertical model.

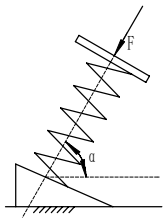

Fig. 3. Tilted model for jumping robot

Suppose the robot will not slide on the ground before jumping. If we neglect the air resistance, the motion of the system is a projectile motion. Then the jumping height (h), distance (d), and their relation are:

$$h = \frac{\eta E_0 \sin^2\alpha}{(m_1+m_2)g} \tag{10}$$

$$d = \frac{2\eta E_0 \sin 2\alpha}{(m_1+m_2)g} \tag{11}$$

$$d = 4h\cot\alpha \tag{12}$$

where η and E_0 are the conversion efficiency and energy stored in the spring respectively as defined in the vertical model. From (12), we can see that different height and distance ratio can be obtained by changing α. Moreover, although the tilted model is different from the vertical one, the three design guidances still hold as can be seen from (10) and (11).

III. DESIGN AND IMPLEMENTATION

Applying the two-mass-spring system to the robot, we come up with a design shown in Fig. 4. Since the compression length cannot be very large due to the robot size, two springs are used according to design guidance one. Aside from the two springs, the other parts can be classified into two sets corresponding to the lower and upper mass in the two-mass-spring system. The deep gray set is the lower mass, while the light gray set is the upper mass. The lower mass, guided by two legs built from a single shaft, can move up and down in the upper mass. The legs are connected to two feet, and the tilted angle can be adjusted by changing the angle between them.

The choice of appropriate spring constants are derived from (10) and $E_0 = K\Delta x^2/2$:

$$K = \frac{2(m_1+m_2)gh}{\eta \sin^2\alpha \Delta x^2}$$

where $\alpha = 80.5^\circ$ can be obtained from (12) by plugging design specifications $h = 15cm$ and $d = 10cm$. As our initial design, let $\Delta x = 12mm$, $\eta = 0.5\,(r = 1)$(Bigger η can be used, but we use 0.5 to leave some margins), then we can get the spring constant $K = 1049N/m$. Thus we choose the spring with a constant $K = 1156N/m$.

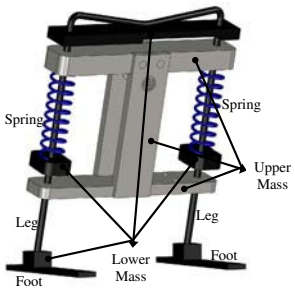

Fig. 4. Solid model for major parts of the robot

As explained in section I, our first goal is to design a robot that can jump once after we randomly throw it. As such, we need two main components in the design. One is the load holding mechanism to keep the compression state after the springs are loaded and trigger mechanism to release the energy stored in the springs. The other is the stabilization mechanism to make the robot ready for jump after being thrown. In this section, the design of these two components will be elaborated.

A. Load holding and trigger mechanism

A bending lever with pivot on the upper mass is used as the load holding mechanism, while a motor actuated cam is adopted as the trigger mechanism. The load and release states are shown in Fig. 5(a) and Fig. 5(b) respectively. The bending lever goes across the upper mass from the front to the back. A roller bearing is attached to the upper end of the lever, which changes the sliding friction between the lever and the holder to rolling friction after trigger.

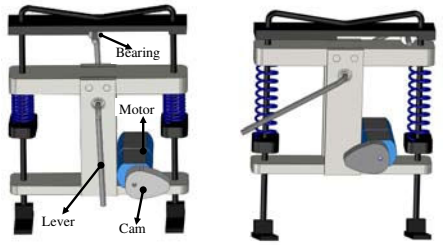

(a) Load state (b) Release state

Fig. 5. Illustration of load holding and trigger mechanism

The holder is a rectangle bar with a rectangle groove. A detailed front view of the holder and lever with bearing is shown in Fig. 6. Note that one side of the groove is near the center of the holder. At load state, the lever's upper end contacts the center side of the groove, while the lower end contacts the cam. Cam's rotation will push the lever's lower end, resulting the release of energy. Note that the horizontal part of the leg is bent to the concave shape shown in Fig. 6, which can share part of the load force from the holder.

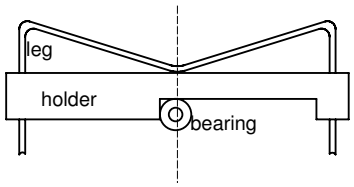

Fig. 6. Detailed view of the holder and relevant parts

B. Stabilization mechanism

The robot feet should always contact the ground before jumping; thus, self-stabilization is needed after we randomly throw it. The ideal choice is to use a hollow sphere to encircle the whole mechanism. By making the center of mass (CoM) of the robot as close as possible to the feet, we can achieve such a stabilization. This principle is similar to a tumbler. A sphere, however, is difficult to be assembled to the jumping mechanism. Hence we use a round pipe plus two polyurethane hemisphere foams on both ends of the pipe to encircle the mechanism. The whole structure is shown in Fig. 7. Note that the feet should be tangent to outer surface of the pipe which is necessary for self-stabilization. Moreover, since the upper mass moves up and down during jump, the stabilization part can only be attached to the lower mass, resulting an increase of the mass ratio. The jumping performance will thus degrade, and the degradation will be analyzed in next section.

During the landing process, the robot can always make the pipe contact the ground because of the round foam. As a result, to achieve stabilizing the robot with the pipe on the ground, the length of the foot is critical. Obviously, if the foot is sufficient long, the robot cannot return to the stabilization state no matter how close the CoM is to the foot. Thus there exists a critical length that the foot cannot exceed. This idea is shown in Fig. 8. Three rolling states: left critical (LC), foot on ground (FoG), and right critical (RC) are shown in the figure. The bold line represents the foot, the circle represents the round pipe, and M is the location of the CoM.

A moving frame is attached to the foot with origin at tangent point of the foot with the circle, X horizontal, and Y vertical in the FoG state. Divide the foot into two parts with length l_1 and l_2 as shown in the figure. The two critical states correspond to when the gravity passes the two foot ends. Take the LC state for example, if we want the robot to turn clockwise, M should be on the right of the foot's left end. Thus when M pass through the left end, l_1 is a critical length. Similar arguments can be applied to the RC state.

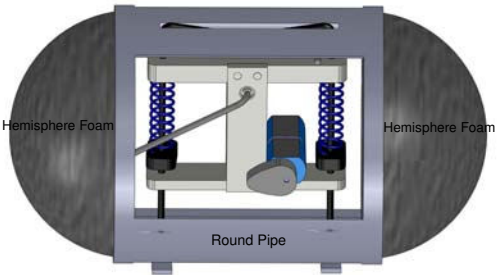

Fig. 7. Whole solid model with self-stabilization parts

Suppose $M=(a,b)$ and the radius of the pipe is r. Since the derivation of l_1 and l_2 is the same, we only consider l_2. Redraw the RC state as shown in Fig. 9, where C is the center of the pipe and B is the tangent point for the pipe and ground. Then l_2 is the length of OA.

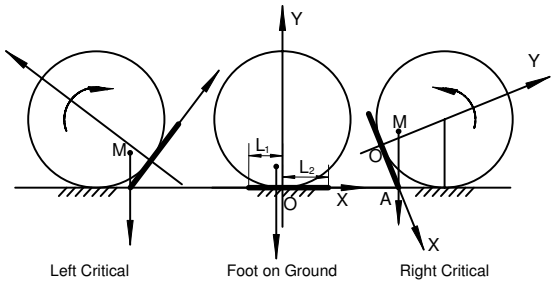

Fig. 8. Self-stabilization illustration with two critical states

Suppose $A=(x_0,0)$, then the slope of MA is $b/(a-x_0)$. Since CB is parallel to MA and BA is perpendicular to it, we can get their equations as:

$$CB: \quad y-r=\frac{b}{a-x_0}x$$
$$BA: \quad y=-\frac{a-x_0}{b}(x-x_0)$$

Point B can be obtained either by intersection of above two lines or by intersection of line CB with the circle. Equating the x coordinate of B by these two methods:

$$b^2X^3-2abX^2+(a^2+2br-r^2)X-2ar=0 \qquad (13)$$

where $X=(a-x_0)/b$. If (13) is solved, we can get $l_2=x_0=a-Xb$. If the robot can jump, the CoM should be within

the range of foot. Thus $a < x_0$, which means $X < 0$. The same equation can be applied to solve for l_1, except that $x_0 < 0$ and $X > 0$. Therefore, given (a,b) and r, we can always determine the length of the foot to make robot self-stabilize. Note that if different takeoff angles are adopted, the coordinates of CoM will be different in the coordinate frame of Fig. 8. Moreover, if the CoM is too high (b is too large), there may not be both a negative and positive solutions to (13), which means we cannot design a foot to make the robot always return to FoG state.

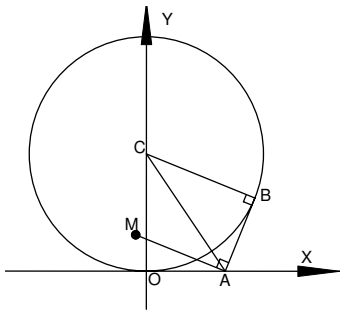

Fig. 9. Right critical state

TABLE I

WEIGHT FOR EACH PART OF THE ROBOT

Part Name	Material	Weight [g]
Lower mass	PMMA/PEEK/Steel	6.5
Upper mass	PMMA	7.7
Cam	PMMA	0.6
springs	Steel	0.8
Lever	Steel	1.8
Round Pipe	Acrylic	9.2
Hemisphere Foams	Polyurethane	3.6
Motor		3.8
Mote		4.4
Lipo Battery		3.5
Total Mass		41.9

TABLE II

PERFORMANCE FOR THREE SITUATIONS

	One	Two	Three
Upper Mass [g]	21.8	21.8	21.8
Lower Mass [g]	6.5	15.7	19.3
Conversion Efficiency [%]	76.9	58.1	52.9
Calculated Height [cm]	43.6	24.6	20.4
Calculated Distance [cm]	46.2	26.3	21.9
Experimental Height [cm]	41	19	15
Experimental Distance [cm]	26	16	11

IV. RESULTS

A. Prototype

Four prototypes have been built as shown in Fig. 1. The robot has a dimension about $6.5cm \times 6.5cm \times 11cm$ and a weight about $41.9g$. In Table I, the detailed weight for each part is listed. Note that the lower mass and upper mass in the table only correspond to the deep and light gray sets shown in Fig. 4, where many other parts are omitted for clear classification. Nevertheless, to compute the jumping performance, all the parts should be classified to the upper mass or lower mass category respectively.

The polymethyl methacrylate (PMMA) is used to construct the upper mass in Fig. 4 because of its low density and high Young's Modulus. Since an inclined hole connecting the feet to the leg is needed, the polyetheretherketone (PEEK), a material less brittle than PMMA, is used to build two feet. Both the leg and lever are built using steel because they need to endure certain loads. The hemisphere foams' weight $3.6g$ is for two of them. The mote in the table, a wireless sensor from Crossbow, is used to control the robot. A motor with rated voltage $3V$, speed $100rpm$, and stall torque $250g.cm$ is employed to trigger the load mechanism. Finally, a $100mAh$ Lipo battery is adopted to actuate the robot.

B. Jumping Performance

If we separate the round pipe and hemisphere foams from the robot, the jumping performance can be evaluated for three situations:

1) with neither the round pipe nor hemisphere foams;
2) with only the round pipe;
3) with both of them.

For these situations, the upper mass is the same, while the lower mass is different because the round pipe, hemisphere foams, or both may attach to it. The calculated performance using the tilted model and experimental performance are shown in Table II. For takeoff angle, although an 80.5° is calculated from specifications in section III, the jumping distance is smaller than expected; therefore, an angle 75° is used instead to meet the design specifications.

The experiment is conducted on a desk by recording a video during the jump, and the performance is obtained by analyzing individual frames. Five frames for each of the three situations are shown in Figs. 10, 11, and 12 respectively. These five frames consist of an initial frame before jump, an upward frame when the robot is going up, a peak frame when the robot is at the highest location, a downward frame when when the robot is going down, and a contact frame when the robot falls on the ground. The experimental values in Table II are read from the peak and contact frame. The jumping height is the vertical location of the foot in the peak frame, while the jumping distance is the horizontal location of center of robot in the contact frame.

As we can see from Table II, the experimental heights are close to calculated ones, while the experimental distances are much smaller. The reason is that sliding between the feet and the desk occurs before the robot begins to jump. Moreover, we cannot make the two feet contact the desk perfectly because of machining error. From the experimental height values for three situations, we can see the height is reduced drastically if the round pipe is added (from $41cm$ to $19cm$). This is due to the large weight of the round pipe which leads to a small conversion efficiency. If, however, we

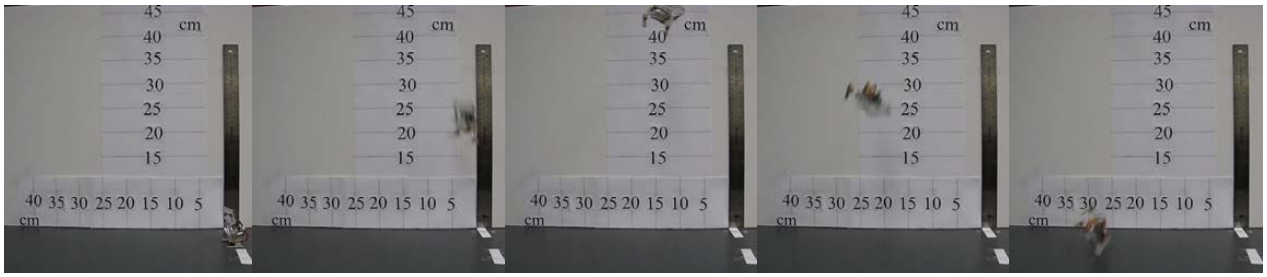

Fig. 10. Jumping sequences with neither the round pipe nor hemisphere foams

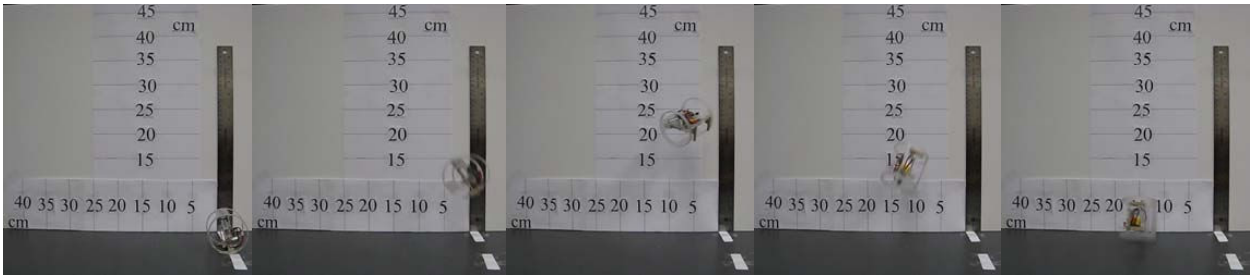

Fig. 11. Jumping sequences with only the round pipe

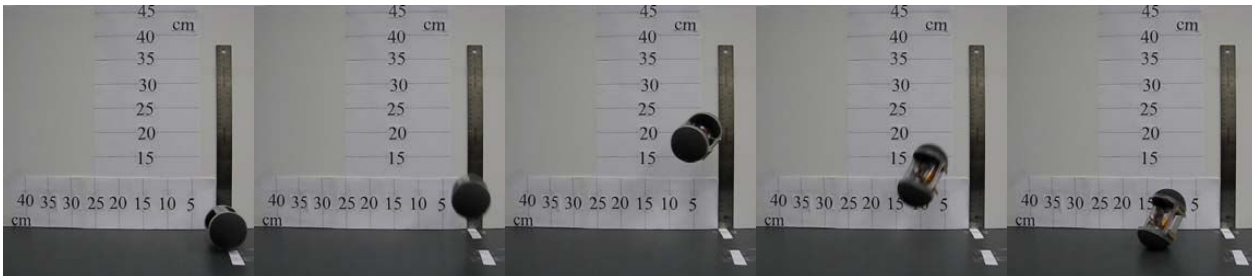

Fig. 12. Jumping sequences with both the round pipe and hemisphere foams

reduce the weight of the pipe, it will be not strong enough to support the robot. Thus a new material with high Young's Modulus and very low density is needed, which can enhance the performance significantly.

V. CONCLUSIONS AND FUTURE WORKS

The development of a jumping robot is presented in this paper. The robot is based on a simple two-mass-spring system. Both the vertical and tilted model of the system are derived, leading to three design principles and the jumping performance formula. After mathematical modeling, detailed design of the robot including the load holding and trigger mechanism, self-stabilization mechanism are elaborated. Experiments for three different situations are performed, and experimental heights match the theoretical calculations well.

Designing an autonomously loading robot will be the major task in the future. To this end, the load holding and trigger mechanism needs to be revised, and the landing and self-stabilization problems in this autonomously loading case also need to be solved.

REFERENCES

[1] A. Howard, M. J. Mataric, and G. S. Sukhatme, "An Incremental Self-Deployment Algorithm for Mobile Sensor Networks," *Autonomous Robots, Special Issue on Intelligent Embedded Systems*, vol. 13, no. 2, pp. 113-126, 2002.

[2] J. Burdick and P. Fiorini, "Minimalist Jumping Robots for Celestial Exploration," *International Journal of Robotics Research*, vol. 22, no. 7, pp. 653-674, 2003.

[3] Z. W. Cen and M. W. Mutka, "Relocation of Hopping Sensors," *in International Conference on Robotics and Automation*, Pasadena, CA, 2008, pp. 569-574.

[4] M. Kovac, M. Fuchs, A. Guignard, J. Zufferey, and D. Floreano, "A miniature 7g jumping robot," *in International Conference on Robotics and Automation*, Pasadena, CA, 2008, pp. 373-378.

[5] U. Scarfogliero, C. Stefanini, and P. Dario, "Design and Development of the Long-Jumping Grillo Mini Robot," *in International Conference on Robotics and Automation*, Roma, Italy, 2007, pp. 467-472.

[6] R. Armour, K. Paskins, A. Bowyer, J. Vincent, and W. Megill, "Jumping robots: a biomimetic solution to locomotion across rough terrain," *Bioinspiration and Biomimetics Journal*, vol. 2, no. 3, pp. 65-82, 2007.

[7] B. G. A. Lambrecht, A. D. Horchler, and R. D. Quinn, "A small, insect inspired robot that runs and jumps," *in International Conference on Robotics and Automation*, Barcelona, Spain, 2005, pp. 1240-1245.

[8] S. A. Stoeter and N. Papanikolopoulos, "Kinematic Motion Model for Jumping Scout Robots," *IEEE Transactions on Robotics and Automation*, vol. 22, no. 2, pp. 398-403, 2006.

[9] F. Kikuchi, Y. Ota, and S. Hirose. "Basic performance experiments for jumping quadruped," *in IEEE/RSJ Int. Conf. Intelligent Robots And Systems*, Las Vegas, NV, 2003, pp. 3378-3383.

[10] Intelligent Mobile Land Mines (IMLM), Sandia National Laboratories, http://www.darpa.mil/sto/smallunitops/shm/sandia.html